The Dynamic Double Layer: Two-Dimensional Condensation at the Mercury–Water Interface

ROBERT DE LEVIE

Chemistry Department, Georgetown University, Washington, D.C. 20057

Received August 25, 1987 (Revised Manuscript Received December 3, 1987)

Contents

Robert de Levie was born in Amsterdam, the Netherlands, and earned his Ph.D. at the University of Amsterdam in 1963. After 2 years of postdoctoral study with Paul Delahay, he joined the faculty of Georgetown University in Washington, D.C. He and his co-workers have worked on various aspects of electrochemistry, including the behavior of porous electrodes, electrochemical oscillators, electrocatalysis, ion transport through lipid bilayers, and two-dimensional phase transitions. Dr. de Levie was the U.S. editor of the *Journal of Electroanalytical Chemistry* from 1970 till 1980.

I. Introduction

Some four decades ago, in a much-quoted contribution to *Chemical Reviews*, David Grahame[1] summarized what was then known about the electrical double layer at the interface between mercury and aqueous electrolyte solutions. Through the work of Lippmann, Gouy, Frumkin, and Grahame, this system had become the paradigm of the electrified interface, a role that it has retained to this day. The picture sketched by Grahame, and since repeated in more recent reviews such as those of Parsons,[2,3] Damaskin,[4] Delahay,[5] and Mohilner,[6] was essentially that of a static interface, which is formed faster than can be resolved experimentally and follows the laws of thermodynamics.

To be sure, there had been some notable exceptions to such a static picture. Gouy, to whom we owe most of our insights in the structure of the double layer, already in 1900 reported that some electrolyte mixtures exhibit "electrocapillary viscosity"[7] and, subsequently, gave its interpretation in terms of diffusion-controlled ion exchange.[8] Later, Frumkin and Melik-Gaikazyan described diffusion-controlled desorption–adsorption peaks.[9] Still, apart from a few cases in which mass transport to and from the electrode was implicated, the general picture for the mercury–solution interface was essentially one of equilibrium.

The earliest indications of the existence of slow double-layer processes came from the work of Lorenz, who reported the phenomenon of capacitive hysteresis in the presence of near-saturated concentrations of nonanoic acid, $CH_3(CH_2)_7COOH$, and interpreted this in terms of film condensation.[10] Shortly thereafter, unusual capacitance "pits" of low, concentration-independent value were observed with several neutral organic substances, including camphor derivatives[11,12] and a number of purines and pyrimidines.[22,23] Soon, many more systems exhibiting symptoms of two-dimensional condensation of neutral compounds were found. The list now includes fatty acids,[10] camphor and related compounds,[11-21] purines, pyrimidines and their derivatives,[22-73] pyridine and bipyridines,[74,75] thiourea,[76-81] quinolines,[82-95] ouabine,[96] tribenzylamine,[97] lipids,[98-103] and coumarin.[104-106]

Shortly after the Lorenz paper, Frumkin and Damaskin[107] reported a slow but pronounced lowering of the interfacial capacitance of mercury in contact with tetrabutylammonium iodide in aqueous 1 M KI solution. Subsequent reports have included, in addition to tetrabutylammonium salts,[107-109] those of tetraphenylphosphonium[110,111] and tetraphenylarsonium.[112]

Recently, some of the above systems have been studied in greater detail by Gierst, Buess-Herman, and others in Brussels and by my co-workers at Georgetown University. A coherent picture has now emerged of two-dimensional phase formation, including the kinetics of phase formation, its statistical mechanics and thermodynamics, and some properties of the films so formed.

Below we will summarize the most salient of these findings, to complement the static picture of the electrified interface painted earlier.[1-6] Most of our examples will deal with the adsorptive behavior of neutral organic

0009-2665/88/0788-0599$06.50/0 © 1988 American Chemical Society

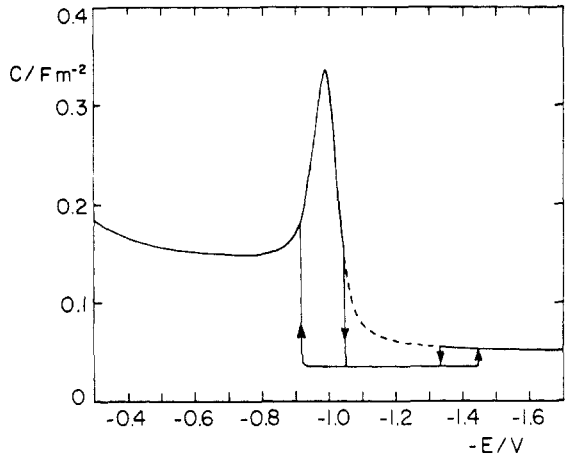

Figure 1. The interfacial capacitance of mercury in contact with 0.1 M $NaClO_4$ + 0.01 M coumarin, as measured at 15 °C at 1.2 kHz, while scanning the bias voltage at a rate of 4.5 mV s^{-1} in either direction. (In the regions of hysteresis, the scan direction is indicated.) The dashed line indicates the (metastable) capacitance measured immediately after a voltage step from outside to inside the pit region. Potentials measured with respect to a mercury/mercurous sulfate electrode in 0.5 M Na_2SO_4. After ref 105.

compounds, dissolved in aqueous electrolyte solutions, at the interface of such solutions with mercury. Subsequently we will briefly describe similar behavior observed with hydrophobic ions.

Some of the stochastic aspects of electrochemical phase formation were summarized recently.[113] The subject of the present review has also been considered by Buess-Herman[114] from a somewhat different perspective.

II. General Aspects of Film Condensation

Some typical features of capacitance pits and the associated hysteresis are illustrated in Figure 1. Usually, the transitions leading into the pit depend on the rate at which the potential is changed, are clearly unidirectional, and exhibit kinetics characteristic of nucleation and growth of a two-dimensional phase. On the other hand, the transitions leading out of the pit are independent of the scan rate and can be traversed in both directions, as long as one does not entirely leave the pit, i.e., as long as at least one cluster remains present. These outer edges of the capacitance pit thus reflect regions of coexistence between the "normal" metal–solution interface and that containing a condensed film. The outer edges of the capacitance pits delineate the region of stability of the condensed film and will be considered in the discussion of the statistical thermodynamics (see section VII).

The capacitance in the pit region is usually quite low and is essentially independent of the concentration of the adsorbate (except near its very edges). Often, the capacitance in the pit is also virtually independent of the applied potential and of temperature. In those cases in which a thermodynamic analysis has been made, interfacial excesses of about (2.0–2.5) × 10^{18} molecules per m^2 have been found (see Table I). Such values are consistent with monolayer films. The width of the pit region depends very strongly on adsorbate concentration and temperature, as well as on the nature and concentration of the electrolyte used.

TABLE I. Molecular Areas Reported for Condensed Films As Determined from (Maximum Bubble Pressure) Measurements of the Interfacial Tension

adsorbate	molecular area, Å²	μmol per m²	ref
camphor	42	4.0	17
borneol	39	4.25	19
adamantol	42	4.0	19
uracil	40	4.2	38
5-methyluracil (=thymine)	39	4.2	38
5-methyluracil (=thymine)	45	3.7	69
1,5-dimethyluracil	43	3.9	38
5,6-dimethyluracil	52	3.2	46
1,5,6-trimethyluracil	48[a]	3.5[a]	46

[a] Limited precision.

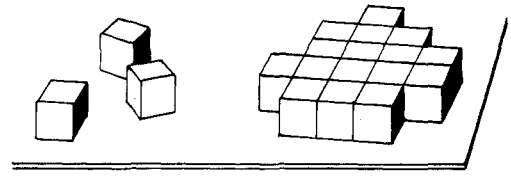

Figure 2. Schematic representation of "normal" adsorption, in which the adsorbate molecules (here depicted as cubes) are randomly oriented in the interface and are surrounded on five sides by the solution (left), and of a two-dimensional condensed adsorbate film (here shown as a small cluster only), in which the adsorbate molecules have up to four adsorbate molecules as nearest neighbors (right).

In the "normal" adsorption of an organic compound at the metal–solution interface, the organic molecule makes contact with the electrode but is, otherwise, still mostly surrounded by the solvent. When we depict the adsorbate molecules schematically as cubes on a flat electrode surface, then they will share one side with the electrode and five with the solvent and its electrolyte ions. In such a situation, the first layer of molecules at the interface still contains both solvent and electrolyte ions, and the interfacial excess of the organic material never quite reaches a value in which all solvent has been displaced from the interface. On an atomically smooth metal such as liquid mercury, the adsorbed organic molecule probably has considerable mobility in the adsorption plane.

In contrast, when a monolayer film is formed through a two-dimensional phase transition, then the organic molecules (still considered schematically as cubes) are most likely surrounded on four sides by similar molecules, while making contact with the electrode and the solvent on one side each (see Figure 2). This is not to imply that solvent molecules (or even electrolyte ions) may not be incorporated in the monolayer but, if they are, it will be like water of crystallization, serving as bridges between adsorbed organic molecules and/or as space fillers, with a more or less defined stoichiometry.

The difference between condensed monolayer films and those formed by polymerization is, of course, that the condensed films do not have covalent bonds between their constituent molecules; i.e., the two-dimensional molecular aggregation is based on weaker cohesive forces, such as hydrophobic and dipole/dipole interactions or, at most, hydrogen bonding. On the other hand, a condensed phase sandwiched between two liquids can be expected to have relatively few structural defects or "pinholes", especially if the film itself is also fluid or, at least, monocrystalline.

III. Stochastic Observations of the Phase Transition

Depending on the relative rates of the condensation process and on experimental conditions such as electrode area,[57] the phase transition can show *deterministic* or *stochastic* behavior. In a typical stochastic response, a single nucleus is formed, which then expands to cover the entire electrode–solution interface. The formation of the single nucleus must be a sufficiently rare event, and subsequent growth sufficiently fast, to reduce the probability of formation of a second nucleus while there is still bare metal–solution interface available. Since the probability of forming a nucleus is directly proportional to the bare interfacial area, the probability of nucleation decreases with decreasing electrode size. Furthermore, the smaller the electrode, the faster it can be covered by a growing nucleus, so that the "window of opportunity" for subsequent nucleation can be closed more quickly. Since both effects work in the same direction, it is sometimes sufficient to reduce the interfacial area by just 2 orders of magnitude to change the observed behavior completely from deterministic to stochastic.[57]

Stochastic phenomena occur without strict reproducibility. For good reasons, chemists have learned to distrust nonreproducible observations; yet here they occur not as the result of some poorly controlled experiment but as the inherent characteristic of observing rare events. However, even though the observations themselves are stochastic, the underlying probabilities are perfectly deterministic and well defined. It is therefore imperative to use statistical analysis to find these probabilities, in order to make sure that experimental artifacts are not dominating the results.

Nucleation, like radioactive disintegration, involves a *continuous* experiment (i.e., it can occur at any time) with a *discrete* outcome, and can therefore be expected to follow a distribution based on Poissonian statistics. This is in contrast to, say, throwing dice, where both the experiment and its result are discrete: one can neither throw 2.5 times nor throw that many eyes. In that case, the statistics must be modeled after the binomial distribution. Nucleation statistics are, also, quite distinct from those involved in measuring one continuous property (such as a current or an absorbance) as a function of another continuous parameter (e.g., voltage, concentration, or time), in which case the Gaussian distribution is the appropriate prototype.

Quantitative stochastic observations are time-consuming because they require a large amount of experimental repetition in order to yield sufficient data for valid statistics. When simple Poissonian statistics apply, the relative standard error in the result is equal to the inverse square root of the number of observations, so that 100 repeated observations still yield relative standard errors of 10%! One might think that the remedy is simple: automate the measurements and repeat them 10000 times instead. Unfortunately, such a strategy often fails. The reason we can sometimes observe stochastic behavior in the first place is, of course, that nucleation is a kinetically highly hindered process. Any spurious pathway that facilitates it will lead to faster nucleation and, hence, will obscure the sought statistics. Quite often, the support of the electrode (e.g., the capillary from which the mercury is suspended) will provide an edge that can function as a site for faster nucleations, often especially after some time has elapsed in the experiment. It is not clear whether the extra nucleation center is a dust particle stuck between the mercury and the glass capillary, a rough spot in the glass edge, a persistent remnant of a previous film, or what, but one often observes that the nucleation process gradually, or suddenly, becomes faster. This effect can be reduced, although often not eliminated entirely, by rigorous purification of the cell and of all chemicals used and, in the case of mercury, by repeated drop formation and dislodgment between repeat experiments. We have found that the data quality is often noticeably improved by charcoal treatment of the electrolyte solution and, if feasible, sublimation of the organic compound.

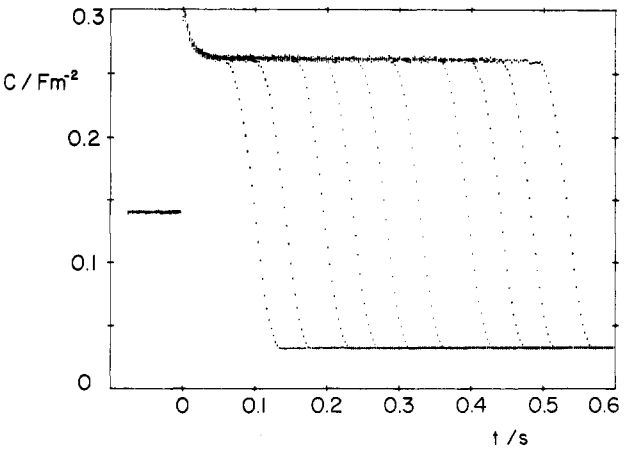

Figure 3. A sampling of capacitance transients obtained during 400 repeat voltage step experiments on individual mercury drop electrodes, following a potential step from −0.7 to −1.0 V. All other conditions are as in Figure 2. From ref 105.

Since the systems discussed here exhibit no faradaic reactions, with their telltale electric currents, the only available experimental "handle" on the condensation kinetics is the measurement of the interfacial capacitance, interfacial charge density, or interfacial tension. Of these, the capacitance is the more readily measurable and has mostly been used, although the Brussels group has demonstrated that charging currents can yield fully equivalent results. Figure 1 illustrates a typical capacitance–potential curve for a system exhibiting film condensation, and Figure 3 shows a corresponding capacitance–time transient following a potential step from outside to within the region of film stability. Immediately after the potential step, the capacitance exhibits a "virtual" level that seems to continue the "normal" capacitance in the absence of a pit. This virtual capacitance is observed as long as nucleation has not yet had time to occur. Once a nucleus is formed, it will quickly expand and cover the interface, thereby reducing the capacitance. The resulting capacitive transient stops once the entire interface has been covered with a monolayer, except when subsequent polylayer formation occurs, an occasional complication discussed in section IX.

In order to extract the moment of nucleation from a transient such as shown in Figure 3, the growth transient must be analyzed. First, the capacitance C is used to calculate a partial film coverage

$$\theta = (C_0 - C)/(C_0 - C_\infty) \quad (1)$$

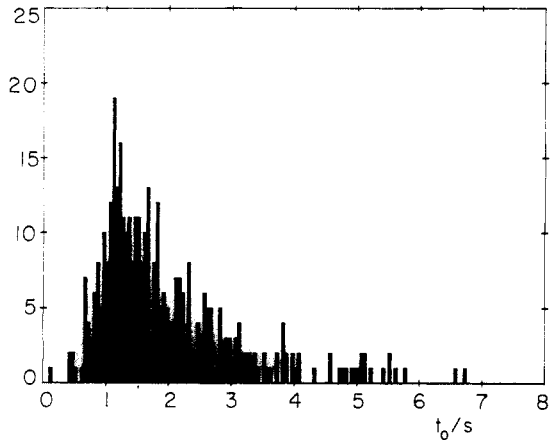

Figure 4. Nomogram showing the number of measurements (out of a total of 400) at which nucleation started in a given interval of 50-ms width. Data from voltage step measurements illustrated in Figure 3; t_n values obtained with eq 2. From ref 105.

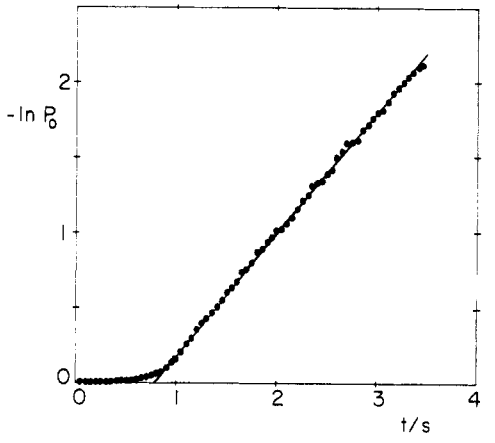

Figure 5. Plot of $-\ln P_0$ versus time t, where P_0 represents the probability of no nucleation up to the time t, as calculated from the data shown in Figure 4. After ref 105.

where C_0 and C_∞ are the capacitance values before and after the transient, respectively. Using a simple model for film growth proportional to the length of the periphery of a growing spherical cap,[88] one can derive the linearized expression

$$\arccos(1 - 2\theta) = (t_n - t)\, v_g/r \qquad (2)$$

Since a hanging mercury drop is near-spherical, with radius r, and essentially edge free, the experimental data thus yield both the film growth rate v_g (from its slope v_g/r) and the moment of nucleation t_n (from its intercept, i.e., by back-extrapolation to $\theta = 0$).

The growth transient is deterministic, because a macroscopically observable capacitance change during growth must involve the incorporation of many thousands of molecules. Thus, the growth curves of repeat experiments should all yield the same growth rates as, indeed, they do. However, the moments of nucleation vary, and these are the ones that must be analyzed statistically. The bar graph of Figure 4 illustrates a set of raw nucleation data resulting from the analysis of some 400 capacitance transients, and Figure 5 shows the resulting probability P_0 that no nucleus has yet been formed at the interface after a given time t. (Since the formation of a second or third nucleus can be masked by the first, and thus may escape experimental detection, it is safest to base the statistical analysis exclusively on P_0.)

The resulting probability curve of Figure 5 exhibits two linear regions, one with zero slope. The intercept of the two linear sections defines an *induction time*, and the slope of the second linear segment the *steady-state nucleation rate*. The induction time is a characteristic property of a nucleation process, reflecting the involvement of a number of aggregation steps before a viable nucleus can be formed. For mathematical details of such statistics the reader is referred to a recent review.[113]

The model implied in the above analysis assumes that nucleation can occur with equal probability at any place in the interface. However, as mentioned earlier, spurious nucleation sometimes appears during the measurements. In its most blatant incarnation, it obliterates all stochasticity by causing virtually instantaneous nucleation; in a more pernicious form, it may add a nonzero slope to the initial segment of the curve in Figure 5, for which correction must be made.[70]

Even when the nucleation occurs at a spurious nucleation center, masking all stochasticity, useful data on the growth rate may still be obtainable. With a hanging mercury electrode, the only special place that remains from drop to drop is the edge where the glass capillary meets the exposed electrode–solution interface. For the usual hanging mercury drop electrode, the area covered by this edge, i.e., the cross-sectional area of the capillary, is much smaller than the total exposed interfacial area and, therefore, acts much like a point source for nucleation. Multiple nuclei formed at that edge will quickly merge as they grow and cover the region around this edge, so that subsequent growth is indistinguishable from that of a single nucleus. This allows one to obtain the growth rate constant, which, under favorable conditions, can be combined with the results of deterministic measurements to deduce the nucleation rate.[64,137]

In order to obtain nucleation and growth rate *constants* rather than their respective rates, one must know the interfacial concentration (or excess) of the adsorbate at the potential used. This requires interfacial tension data, which are difficult to obtain for film-forming systems, and which could, conceivably, be gotten from chronocoulometric experiments when the adsorbate is either reducible or oxidizable at some other potential.

IV. Deterministic Observations of the Phase Transition

Although deterministic behavior has been observed much more often, we describe it only now, after a discussion of the stochastic response, because it is inherently somewhat more complicated. The additional complexity stems from the competition of numerous growing nuclei for the limited interfacial area and, often, also from the continued formation of new nuclei. Whether the second complication arises depends, at least partially, on the experimental conditions: the distinction between "instantaneous" and "progressive" nucleation[115] often merely reflects the experimental protocol used, in which case it conveys no information regarding the system studied.

The simplest situation is one in which one generates a fixed number of nuclei at a given moment and then observes the subsequent growth of these nuclei. Such

instantaneous nucleation can readily be achieved with a double potential step which, starting at a potential E_1 outside the range of film formation, first brings the potential to a value E_2 where nucleation is rapid, and then backs off to a potential E_3 at which nucleation is highly unlikely but growth of already-formed nuclei is still favored. The dwell time at the nucleation potential, E_2, can be chosen to be so short as to be insignificant on the time scale of the resulting capacitance transient, so that this transient exhibits neither the capacitance at the nucleation potential E_2 nor a delay time at the development potential E_3. When the nucleation pulse is also short enough, so that growth at that potential is still insignificant, all resulting nuclei will grow as if they were born at the very same moment.

The data analysis now must take into account the fact that there are numerous nuclei expanding simultaneously until they touch and mutually inhibit further growth. A mathematical analysis of the overlap of randomly placed circular nuclei was first given by Canac[116-120] and can be used to correct for such overlap. The Canac equation

$$\theta = 1 - \exp(-\theta_x) \quad (3)$$

shows that the experimentally accessible covered fraction θ of the interface can readily be converted into that area fraction, θ_x, that would have been covered in the absence of overlap. The resulting double-logarithmic Avrami plot of the extended area fraction θ_x versus time t then contains the product of the number of nuclei generated during the nucleation pulse at E_2 and the growth rate at the development potential E_3.

In the absence of a separate nucleation pulse, nucleation and growth will occur side by side during the entire transient. The corresponding capacitance transient will display a delay time resulting from nucleation, similar to that in Figure 3, although the entire curve will now be perfectly reproducible. The Canac equation is still applicable, as it is independent of time and of the relative sizes of the nuclei, and the Avrami plot will now reflect the combined time dependences of nucleation and growth. As already mentioned, it may sometimes be possible to resolve the corresponding nucleation and growth rates by using growth rates determined independently from experiments showing edge nucleation.

V. Film Composition

The above kinetics of interfacial condensation are compatible with the formation of two-dimensional films but do not provide any direct information on film composition or molecular orientation. Often, the film capacitance is independent of the nature and concentration of the electrolyte used, suggesting that the film does not contain electrolyte ions. Similarly, the film capacitance is usually independent of adsorbate concentration, as one would expect for a condensed monolayer. However, these observations would not exclude either the inclusion of a stoichiometric amount of solvent or the formation of polylayers. Additional experiments are therefore required to settle the nature of the film.

Interfacial tension measurements have been made, using the maximum bubble pressure method,[121-124] which may be somewhat more trouble-free than the Lippmann electrometer in the case of film formation. Nevertheless, it is often difficult to obtain reproducible interfacial tension measurements, even when special precautions are taken to nucleate the film. (The very small electrode area exposed in a maximum bubble pressure capillary, with a typical radius of less than 10 μm, may make nucleation of the film stochastic. During the early phase of the measurement, the electrode is therefore best kept at a potential in the middle of the capacitance pit, where the nucleation rate is maximal, in order to ensure film formation.)

In those cases for which interfacial tension measurements have been reported, they have clearly indicated the formation of a monolayer (see Table I). The precise molecular orientation in such a layer poses a more difficult problem. While the distinction between a monolayer and a polylayer is, essentially, a binary question, which does not require very high data precision, the determination of molecular orientation from interfacial excess alone is a tricky business, relying heavily on the precision of the interfacial excess data and, also, on the methods used to estimate molecular area. For example, Brabec et al.[38] determined the molecular area of thymine in the pit region as 39 Å^2. Comparison with the dimensions of a tightly fitting rectangular box, drawn around a molecular model based on van der Waals radii, then led them to conclude that thymine is adsorbed with its plane perpendicular to the interface. We redetermined the molecular area as 45 Å^2 and concluded that thymine was lying flat on the electrode,[69] based on comparison with a published crystal structure in which thymine forms hydrogen-bonded planes in which each thymine molecule occupies 44 Å^2.[125] Molecules seldom pack as rectangular boxes. Moreover, in cases in which the possibility of multiple hydrogen bonding must be anticipated,[126] use of van der Waals radii can lead to further overestimation of the spatial requirements.

There still remains the question of the intermolecular forces responsible for film condensation. In the case of camphor, a rather rigid, near-spherical molecule with a single carbonyl group, or that of the essentially planar coumarin with both a ring oxygen and a carbonyl group, dipolar interactions are the most plausible; in the case of thymine, hydrogen bonding is likely if the orientation is as envisioned by Saffarian et al.[69]

Whether a condensed film should be considered a two-dimensional liquid or solid is not so easy to determine: it depends, of course, on how one defines liquidity or solidity in this case. A possible distinction might be found by considering the shape of a growing nucleus: does it tend to minimize its periphery, as a drop of liquid, or does it show facets reflecting a molecular lattice, as a crystal? Unfortunately, the growth transients are rather insensitive to the difference between a growing circle or square, and it would be even more difficult to distinguish a circle from, say, a regular hexagon or octagon. We note in this context that the earlier mentioned method to correct for overlap[116-120] applies, strictly speaking, only to patches that retain their original shape upon contact, i.e., to "solid" films. It is not known how much different the predicted result would be if, upon contact, the patches were to coalesce, retaining their area while reducing the lengths of their growing peripheries. Therefore it is impossible to judge

whether the good adherence of the experimental data to the Canac formalism can be used to distinguish between solid and liquid films.

Another criterion to distinguish between a liquid and a solid film might be found in the dissolution kinetics. We have not yet discussed these, but they are often either exponential or follow the equation for mononuclear growth. If the film were liquid, one might anticipate that film dissolution would require the "nucleation" of an opening in the monolayer, in which case the dissolution transients would run polynuclear growth in reverse. No such transients have yet been reported, but neither has a satisfactory explanation been found for the most prevalent, exponential dissolution transients. If the edge near the capillary can act as a nucleation center, dissolution might exhibit the transient behavior of reverse mononuclear growth, as sometimes observed. For a solid, on the other hand, one would expect that monolayer films grown in deterministic nucleation experiments, i.e., from multiple nuclei, would still retain their original molecular orientations and form crystal domains. The grain boundaries in such films would be expected to be the places where dissolution could start.[127] However, it is not clear why such dissolution along grain boundaries should lead to exponential dissolution transients. An exponential dissolution transient would, of course, result when the molecules in a liquid film were to leave it randomly, in which case the dissolution rate would simply be proportional to the area fraction covered by the film, but it would seem unlikely that molecules at edge sites would not dominate the dissolution process.

Finally, at a more conceptual level, the question under discussion here may not even be answerable in principle. The basic difference between a liquid and a solid lies in the long-range order of the solid. Peierls[128,129] and Mermin[130] have argued that conventional long-range order in a two-dimensional solid cannot exist, and this argument should apply also to supported films as long as these are noncommensurate with their supporting substrate.[131] Thus, the question whether the condensed monolayer film behaves as a solid or a liquid may not have a general answer and, at any rate, is as yet unresolved.

Regardless of the above question, condensation phenomena depend not only on molecular *interactions* but also on considerations of molecular *packing*. Thus it is perhaps not surprising that an example has recently been reported in which the nature of the electrolyte cation is critical for the formation of a condensed film.[72] In this case, sodium ions (but neither Li^+ nor K^+) appear to be incorporated in a condensed monolayer of 6-methyluracil, possibly structuring it through hydrogen bonding by its coordinating water. This example indicates that one must be careful not to overstate the apparent independence of pit capacitance on electrolyte concentration: the film may always contain a fixed amount of solvent molecules and electrolyte ions, in which case its capacitance would not vary with salt concentration.

VI. Thermodynamics

The thermodynamics of the electrified interface, in the absence of charge transfer, go back to Lippmann[132] and can be based solidly on Gibbsian principles.[133,134]

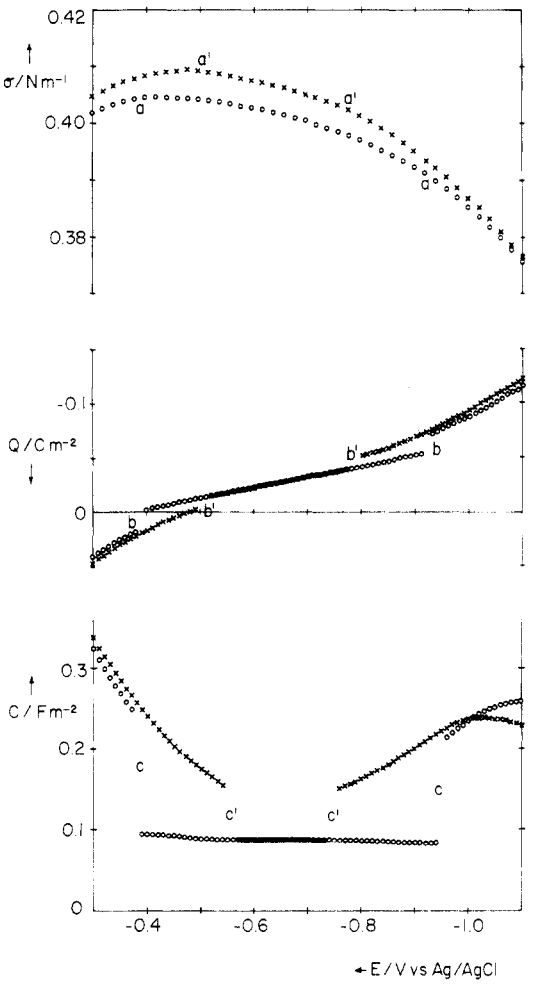

Figure 6. Three independent measurements of the interfacial tension σ, the charge density Q, and the interfacial capacitance C of mercury in contact with 1.0 M NaCl + 24.7 mM thymine (circles) or 15.0 mM thymine (crosses) at 25 °C. All potentials are with respect to an internal Ag/AgCl electrode. The interfacial tension was determined with a maximum bubble pressure instrument, the charge density from the polarographic charging current, and the capacitance with hanging mercury drops and voltage step measurements with a superimposed 300-Hz sine wave. The onset of interfacial condensation at a and a′, respectively, is barely discernible from the interfacial tension; it should show as smooth transitions at b and b′ in the charge density (but is not seen here because the data analysis method used is not valid in the coexistence region) and as sharp peaks at c and c′ in the capacitance (if the latter were measured at a sufficiently low frequency). After ref 69.

They relate the three principal thermodynamic quantities, interfacial tension σ, charge density Q, and interfacial capacitance C, through

$$C = -(\partial Q/\partial E)_{P,T,\mu} = -(\partial^2\sigma/\partial E)_{P,T,\mu} \qquad (4)$$

where E is potential, P pressure, T temperature, and μ chemical potential. C, Q, and σ can be determined from independent measurements,[69] and the relations of eq 4 are then found to hold in the pit region as well as outside it (see Figure 6). This may come as a surprise because, in the pit region, we have three physically distinct phases: the metal, the monolayer film, and the aqueous solution. However, a two-dimensional film is not a separate phase in a thermodynamic sense, since it has no bulk properties. This apparent applicability of classical thermodynamics, even when an interposed condensed monolayer separates the two bulk phases,

has made it possible to determine the monolayer nature of the film by calculating the corresponding relative interfacial excess Γ of the adsorbate A with respect to the solvent S as

$$\Gamma = -(\partial\sigma/\partial\mu_A)_{P,T,E,\mu_{i\neq A,S}} \quad (5)$$

The thermodynamically most intriguing regions are those of partial film coverage, in which the condensed film coexists with an interface exhibiting noncondensed adsorption. Such coexistence regions are found near the pit edges, which, as mentioned already, are not infinitely sharp but have a measurable width (of the order of 0.01 V in the case of thymine). The interfacial tension is a direct measure of the interfacial energy and must, therefore, be a continuous function of potential as, indeed, it is (see Figure 6). There is no problem relating Q and σ in Figure 6 through eq 4. The dynamic method used to measure Q is not applicable to the coexistence regions, so that the precise shape of the charge density–potential curve in those regions has not been determined so far. However, even when what appear to be discontinuities at b and b′ in Figure 6 are connected smoothly (as they must be, in view of the continuity of the interfacial tension curve) in the region of coexistence of noncondensed and condensed phases, the differentiation of the charge density should lead to very pronounced peaks on the capacitance curves of Figure 6 at c and c′. The reason such capacitance peaks are usually not observed is the following.

When one moves from one potential to another inside a coexistence region, the capacitance (as measured with an audio-frequency signal) follows, but relatively slowly. Even though no nucleation limitation is involved, film growth or shrinkage (negative growth) can still be a relatively slow process, especially in the coexistence regions, where it typically exhibits characteristic times of the order of a few to many seconds. The corresponding peaks can therefore be expected to be observable mostly at quite low (typically, subhertz) frequencies and are, consequently, lacking from audio-frequency capacitance measurements such as those of Figures 6 and 7.

Nucleation is often so slow that it is possible to observe, at potentials in the pit region, the capacitance or charge density before appreciable condensation has taken place. These metastable, "virtual" capacitance values can be integrated to yield the corresponding metastable interfacial tension (see eq 4), which subsequently, at least in principle, can be differentiated to give the metastable interfacial excess, using eq 5.

When the difference $\Delta\sigma$ in interfacial tension between the condensed and the noncondensed states (at constant potential, temperature, pressure, and solution composition) is introduced in the classical nucleation theory,[135–138] the nucleation rate J can be expressed as

$$J = J_\infty \exp(\pi\epsilon^2/kT\Delta\sigma) \quad (6)$$

where J_∞ would correspond to the nucleation rate for $\Delta\sigma \rightarrow -\infty$, ϵ is the line tension between condensed and noncondensed regions, and the factor π reflects the assumption of circular clusters. Here, then, the interfacial tension gap $\Delta\sigma$ is seen as a driving force in the nucleation kinetics.[127,139] As just mentioned, this interfacial tension gap can be estimated by integration from the difference between the stable and metastable charge densities, starting from a potential of coexistence, E_c, where $\Delta\sigma$ must be zero.

Usually, both charge density–potential curves are near-linear over small ranges of potential. In that case, $\Delta\sigma$ is directly proportional to the potential difference $E - E_c$. When one ignores the dependence on potential of the metastable interfacial excess, which only affects the preexponential term J_∞ in eq 6, then a linear dependence of ln J on $1/(E - E_c)$ is predicted, as indeed observed with quinoline.[64]

VII. Statistical Mechanics

There have been several attempts to describe the formation of two-dimensional condensation in terms of adsorption isotherms,[140–143] e.g., starting from the Frumkin isotherm,[144] which explicitly incorporates a phenomenological term for adsorbate–adsorbate interactions. Here we will describe a quite different approach based on statistical mechanics.

One of the simplest statistical-mechanical models used to describe phase transitions is that first posed by Lenz[145] and solved, in one dimension, by Ising[146] in connection with ferromagnetism. In approaches of this type, now generically called Ising models, all lattice positions are described in terms of a limited number of discrete "states", each associated with a particular "spin" which, in our case, would reflect its occupancy. Usually, one considers spin–spin interactions between neighboring molecules only. It was shown by Ising that such a one-dimensional two-state model could not rationalize the ferromagnetic phase transition.[146] Onsager subsequently derived under what conditions a two-dimensional two-state Ising model predicts a phase transition,[147] while the mathematical complications associated with three-dimensional Ising models seem to have precluded their quantitative study so far. There has been a consequent mismatch between the mathematics of Ising-type phase transitions, which are available for two-dimensional systems, and experimental observations of phase transitions, which, so far, have been confined to three dimensions. Thus the two-dimensional condensation at the metal–solution interface provides an interesting test of the applicability of Ising models.

In an Ising model, one first formulates the Hamiltonian describing the molecular interactions. We consider the simplest possible Ising model, by using only two states: sites are assumed to be occupied by either adsorbate or solvent. Thus we neglect the presence of electrolyte ions and, also, the possibility of different adsorbate and solvent orientations. For molecular adsorption at an electrified interface, where electric field strengths can be extremely high, the primary interactions involve molecular dipole moments and polarizabilities. Furthermore, the chemical potential of the adsorbate reflects the variable adsorbate concentration in solution. Thus, the Hamiltonian H will contain two terms involving the electric field F at the center of the adsorbed molecules, one reflecting the molecular dipole moments p and one depending on their polarizabilities α, as well as one term containing the adsorbate concentration c, which derives from its chemical potential. Furthermore, there are a number of terms which are essentially independent of the major experimental variables, applied potential E, and adsorbate concen-

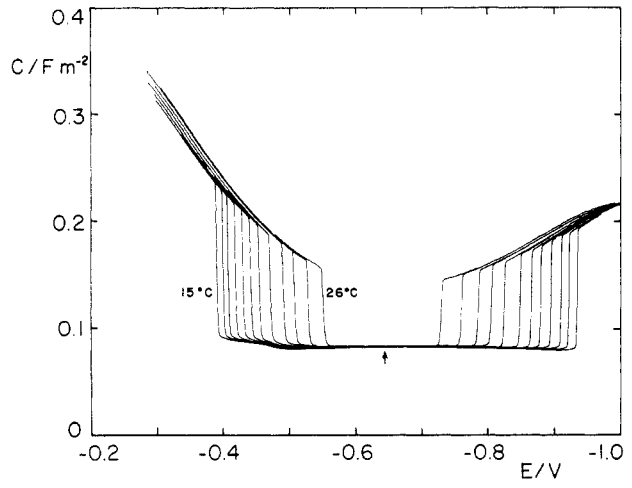

Figure 7. The capacitance pits (measured by very slowly scanning the voltage from the middle of the pit, near the arrow, to avoid hysteresis) in aqueous 1.0 M NaCl + 13 mM thymine at 1 °C temperature increments from 15 through 26 °C. From ref 146.

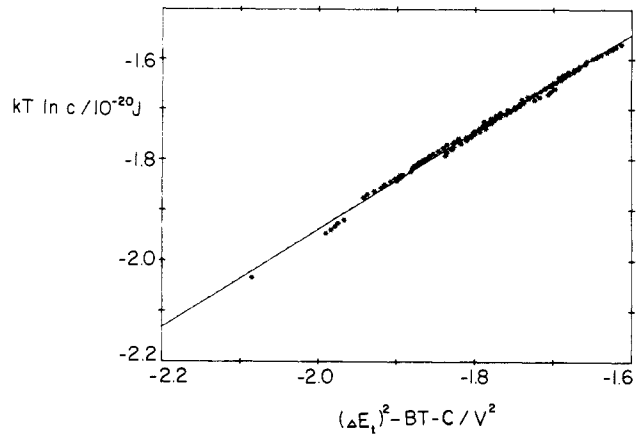

Figure 8. The square of the pit width ΔE_t is a linearly related to $kT \ln c$, where c denotes the thymine concentration (in M) in aqueous 1.0 M NaCl solution in contact with mercury. Composite representation of all 119 values of ΔE_t determined for a range of temperatures and thymine concentrations. B and C are constants. From ref 148, with permission.

tration c, and which can therefore be combined in a constant K, so that

$$H = \tfrac{1}{2}\Delta\alpha F^2 - \Delta p F + kT \ln c + K \qquad (7)$$

where Δp and $\Delta\alpha$ reflect differences in dipole moment and polarizability, respectively, between adsorbate and solvent, and k is the Boltzmann constant.

As Onsager showed, the phase transition occurs when H is zero. At constant temperature and concentration, this yields

$$F = \frac{\Delta p \pm \sqrt{(\Delta p)^2 - 2\Delta\alpha\{kT \ln c + K\}}}{\Delta\alpha} \qquad (8)$$

When $(\Delta p)^2 > 2\Delta\alpha\{kT \ln c + K\}$, there must be two field strengths, F_+ and F_-, at which a phase transition occurs, and these must be symmetrically located around $\Delta p/\Delta\alpha$. Moreover, the square of the difference $F = F_+ - F_-$ should be a linear function of ln c.

When a plausible relation is used to relate the electric field F to the externally applied potential E, a quadratic dependence of the transition potentials (such as illustrated in Figure 7) on temperature and on the logarithm of the adsorbate concentration is obtained, in agreement with experimental evidence.[14,17,55,62,148] Moreover, all experimental data at various temperatures and concentrations can be combined into a single linear relation between the square of the pit width E_t and ln c.[148] An example of such a plot is shown in Figure 8.

The above model is based exclusively on the interfacial properties outside the pit region and, therefore, does not "sense" the nature of the condensed film. Consequently, the model is applicable even when the anodic and cathodic transitions lead to different condensed phases, as in the case of 4,6-dihydroxy-2-methylpyrimidine.[73] When the adsorbate orientations on the anodic and cathodic side of the pit region differ, two distinct sets of parabolas are obtained for the pit edges as a function of temperature or log (concentration).[106]

VIII. Inhibition

The rates of most electron-transfer reactions at the electrode–solution interface are quite sensitive to the presence of adsorbates in the very region in which the electron transfer takes place. Adsorbates can act to enhance the electron-transfer rate, e.g., by forming an electron-conducting "bridge" between the electrode and the electroactive species,[149,150] or to slow them down, e.g., by blocking access to the interface. Moreover, the mere presence of adsorbates will, in general, affect the interfacial charge density and, hence, the potential distribution in the interface and, consequently, the electron-transfer rates.[151] Finally, the interface may be quite inhomogeneous in the presence of noncondensing adsorbents, and one may have to consider different reaction pathways, some involving adsorbate and some not. The combination of these various effects often makes an unambiguous interpretation difficult if not impossible. The situation is somewhat easier in the presence of a condensed monolayer, in which case the interface is, at least, homogeneous. So far, there have only been reports of inhibition of electrode reactions by such films, although rate enhancement may well be observable with the proper choice of adsorbates.

With "simple" electron-transfer reactions, such as the one-electron reductions of Eu(III) or V(III), there is considerable inhibition by an adsorbed condensed thymine monolayer. The interesting aspect here is that this inhibition is independent of the aqueous thymine concentration, as long as the latter is sufficiently high to maintain the condensed film. This is as one might expect, because the composition of the inhibiting film is constant. However, under similar conditions, the inhibition of the two-electron reductions of Pb(II) and Cd(II) increases with increasing bulk thymine concentration.

The distinguishing feature here is not that between one- and two-electron transfers, but between the formation of water- and mercury-soluble reaction products:[95] the lead and cadmium nuclei must cross the monolayer, since their reduced forms disolve as amalgams, whereas only electrons need to cross the film (most likely by tunneling) for the reduction of europium and vanadium. Work must be performed in order to make an opening in the monolayer for the passage of the metal nuclei. Even though the film *composition* is constant, the film *pressure* is not, and this causes the

variation of inhibition with thymine concentration. (In this respect, the thymine film seems to behave as if it were a liquid.) The dependence of the inhibition on the thymine concentration leads to quite plausible estimates of the cross-sectional areas involved.[68]

The inhibition of the one-electron reduction of cobalt(III) hexaammine in the presence of a condensed thymine film also depends strongly on thymine concentration,[68] indicating that its electrode reduction requires that an opening be made in the monolayer. In this case there is, apparently, a need to make physical contact with the electrode before electron transfer can take place. The qualitative dependence of inhibition by a condensed monolayer on the inhibitor concentration thus appears to provide a simple, qualitative criterion for distinguishing between what might be called outer- and inner-sphere interfacial electron-transfer reactions.[68] It remains to be seen whether the above approach has general applicability.

IX. Polymorphism and Polylayer Formation

In several instances, more than one condensed phase can be formed, depending on the applied potential. Sometimes, the two regions in which the corresponding capacitance pits are formed are separated by regions of noncondensed adsorption whereas in other examples (or, sometimes, merely in the presence of a higher adsorbate concentration), the pit regions are adjacent to each other. Transitions from one pit region to the other in the latter case can, again, involve nucleation, indicating that quite different molecular orientations are obtained in the two pit regions.[71,73] Figure 9 illustrates that one can sometimes observe the successive formation of two different condensed phases at a single applied potential.[71] On some occasions, a metastable film may be sufficiently long-lived to allow a comparison between the inhibitions caused by the metastable and stable films. Indeed, the two films may inhibit electrode reactions differently.[73]

In saturated and supersaturated solutions one can also observe deep capacitance depressions, which appear to correspond to the formation of polylayers rather than monolayers.[71] The distinguishing feature here seems to be that no stationary capacitance can be reached. It is possible that a monolayer is formed first, which then forms the substrate for continued three-dimensional growth. Polylayer adsorption had, of course, been recognized much earlier.[152] The observation is mentioned here only to warn the reader that not all capacitance depressions, even those with hysteresis, need to correspond to condensed monolayer films.

X. Ionic Films

The formation of condensed monolayers is not restricted to neutral adsorbates: several examples have recently been found in which similar observations are made in solutions containing adsorbable hydrophobic ions.[107-112] One would expect that, in these cases, *salt* layers are formed, i.e., that the ionic charges of the hydrophobic ions are compensated by coadsorption of counterions. This tallies with the experimental observation that such condensation processes are very dependent on the nature and concentration of the "supporting" electrolyte present. An interesting aspect

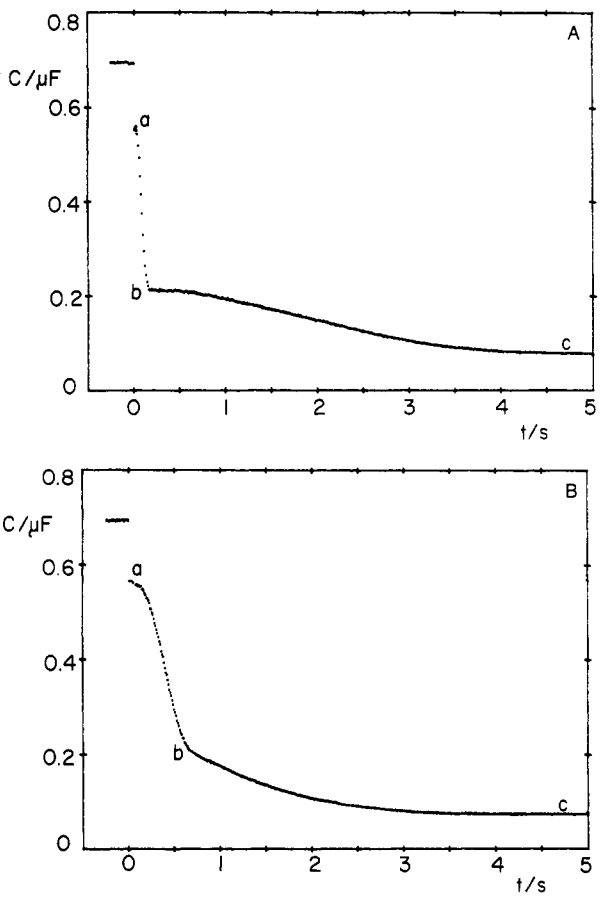

Figure 9. Capacitance transients following voltage steps from −1.100 to −0.950 V (top) and −0.955 V (bottom) in a solution of aqueous 1.0 M NaCl + 26 mM thymine in contact with mercury, at 20 °C, showing two successive nucleation transients, first from the noncondensed state a to the condensed film b and then on to the condensed film c. After ref 71.

is the observation of *two* slow phase-transformation-like processes at relatively low concentrations of the hydrophobic ions, which might possibly reflect the successive formation of two salt monolayers.[109] There is also chronocoulometric evidence for monolayer salt adsorption[153-155] and for the formation of two monolayers.[156]

In single electrolytes, the strong electrical driving force associated with deviations from electroneutrality is responsible for the rapid establishment (typically well within 1 μs) of the double layer. In electrolyte mixtures, electroneutrality requirements can be met by the most abundant ions, while fine-tuning of adsorption interactions can take place at a much lower pace. Most of the above examples of two-dimensional condensation of hydrophobic ions involve electrolyte *mixtures* of a hydrophobic and a nonhydrophobic salt, with the latter in significant excess. In that case, as in the KI + KCl mixture studied by Gouy,[7,8] the interfacial electroneutrality requirements are met initially by the more abundant ions, which can be exchanged subsequently for the more strongly adsorbed ions. Recently, however, an example has been found of phase transitions in a solution of a single hydrophobic salt, in the absence of a "supporting" electrolyte.[111] It is possible that, in this case, the transition occurs at an interface that already carries a salt monolayer,[157] in which case electroneutrality considerations would not affect the condensation process.

XI. Concluding Remarks

We have reviewed the abundance of recent evidence showing that the double layer is not always a static, near-equilibrium system but, sometimes, shows interesting dynamic behavior, associated with two-dimensional condensation, i.e., with the nucleation and growth of monolayer films. Because interfacial concentrations can be controlled with exquisite precision and speed by changing the applied potential and because changes in interfacial structure can be measured simultaneously with great resolution, this relatively recent method of studying nucleation phenomena is among the most powerful ones, especially since it can sometimes provide both deterministic and stochastic measurements.

The usual double-layer thermodynamics for polarizable electrodes appear to apply, despite the presence of an additional third phase: the adsorbed monolayer. The two-dimensional phase transformation also provides an example of the applicability of Ising statistics.

The condensed monolayers inhibit many electrode reactions. Such inhibition appears capable of providing a qualitative criterion to distinguish inner- from outer-sphere electrode reactions. If condensed monolayers can be found with catalytic properties, a most useful model system for studying so-called "modified electrodes" would become available.

The processes discussed here provide many analogies with faradaic processes that involve nucleation, such as underpotential deposition, oxidative film formation such as that of calomel, and electrocrystallization. For example, there are several reports of electrode reactions that proceed only after a monolayer film of reaction intermediates or products has been formed.[158-161] Such systems are, almost inevitably, quite complex. Concepts established with the nonfaradaic and, in many respects, simpler systems described here may well be transferable to their faradaic counterparts and, therefore, helpful in unraveling them.

XII. Acknowledgments

The author gratefully acknowledges the stimulating cooperation of his co-workers, especially Dr. R. Sridharan, Dr. R. Srinivasan, Dr. M. H. Saffarian, and Mr. C. Kontoyannis, and financial support from the National Science Foundation under Grants CHE-8214910 and CHE-8707361.

Registry No. Hg, 7439-97-6; H_2O, 7732-18-5.

XIII. References

(1) Grahame, D. C. *Chem. Rev.* **1947**, *41*, 441.
(2) Parsons, R. *Mod. Aspects Electrochem.* **1954**, *1*, 103.
(3) Parsons, R. *Adv. Electrochem. Electrochem. Eng.* **1961**, *1*, 1.
(4) Damaskin, B. B. *Usp. Khim.* **1961**, *30*, 220.
(5) Delahay, P. *Double Layer and Electrode Kinetics*; Wiley: New York, 1965.
(6) Mohilner, D. M. *Electroanal. Chem.* **1966**, *1*, 241.
(7) Gouy, G. *C. R. Hebd. Seances Acad. Sci.* **1900**, *131*, 835.
(8) Gouy, G. *Ann. Phys. (Paris)* **1917**, *(9)*7, 129.
(9) Frumkin, A. N.; Melik-Gaikazyan, V. I. *Dokl. Akad. Nauk SSSR* **1951**, *77*, 855.
(10) Lorenz, W. *Z. Elektrochem.* **1958**, *62*, 192.
(11) Sherman, E. O., Jr. *Ph.D. Thesis*, University of Illinois, 1963.
(12) Sathyanarayana, S. *J. Electroanal. Chem. Interfacial Electrochem.* **1965**, *10*, 56.
(13) Sathyanarayana, S.; Baikerikar, K. G. *J. Electroanal. Chem. Interfacial Electrochem.* **1969**, *21*, 449.
(14) Baikerikar, K. G.; Sathyanarayana, S. *J. Electroanal. Chem. Interfacial Electrochem.* **1970**, *24*, 333.
(15) Sathyanarayana, S.; Baikerikar, K. G. *J. Electroanal. Chem. Interfacial Electrochem.* **1970**, *25*, 209.
(16) Damaskin, B. B.; Stenina, E. V.; Yusupova, V. A.; Fedorovich, N. V. *Elektrokhimiya* **1972**, *8*, 1409.
(17) Dyatkina, S. L.; Damaskin, B. B.; Fedorovich, N. V.; Stenina, E. V.; Yusupova, V. A. *Elektrokhimiya* **1972**, *9*, 1283.
(18) Frumkin, A. N.; Stenina, E. V.; Nikolaeva-Fedorovich, N. V.; Petukhova, G. N.; Yusupova, V. A. *Rev. Roum. Chim.* **1972**, *17*, 155.
(19) Dyatkina, S. L.; Damaskin, B. B.; Stenina, E. V.; Fedorovich, N. V. *Elektrokhimiya* **1974**, *10*, 318. (a) Stenina, E. V.; Frumkin, A. N.; Nikolaeva-Fedorovich, N. V.; Osipov, E. V. *J. Electroanal. Chem. Interfacial Electrochem.* **1975**, *62*, 11.
(20) Ramamurthy, A. C.; Sathyanarayana, S. *J. Electroanal. Chem. Interfacial Electrochem.* **1976**, *73*, 253.
(21) Sridharan, R.; de Levie, R. *J. Electroanal. Chem. Interfacial Electrochem.* **1986**, *205*, 303.
(22) Vetterl, V. *Experientia* **1965**, *21*, 9.
(23) Vetterl, V. *Collect. Czech. Chem. Commun.* **1966**, *31*, 2105.
(24) Vetterl, V. *Biophysik (Berlin)* **1968**, *5*, 255.
(25) Vetterl, V. *J. Electroanal. Chem. Interfacial Electrochem.* **1968**, *19*, 169.
(26) Webb, J. W.; Janik, B.; Elving, P. J. *J. Am. Chem. Soc.* **1973**, *95*, 8495.
(27) Retter, U.; Jehring, H.; Vetterl, V. *J. Electroanal. Chem. Interfacial Electrochem.* **1974**, *57*, 391.
(28) Vetterl, V.; Kovaříková, E. *Nucleic Acids Res.* **1975**, *1*, S93.
(29) Krznarič, D.; Valenta, P.; Nürnberg, H. W. *J. Electroanal. Chem. Interfacial Electrochem.* **1975**, *65*, 863.
(30) Vetterl, V. *Bioelectrochem. Bioenerg.* **1976**, *3*, 338.
(31) Valenta, P.; Nürnberg, H. W.; Krznarič, D. *Bioelectrochem. Bioenerg.* **1976**, *3*, 418.
(32) Vetterl, V.; Kovaříková, E.; Zaludová, R. *Bioelectrochem. Bioenerg.* **1977**, *4*, 389.
(33) Valenta, P.; Krznarič, D. *J. Electroanal. Chem. Interfacial Electrochem.* **1977**, *75*, 437.
(34) Kinoshita, H.; Christian, S. D.; Dryhurst, G. *J. Electroanal. Chem. Interfacial Electrochem.* **1977**, *83*, 151.
(35) Kinoshita, H.; Christian, S. D.; Dryhurst, G. *J. Electroanal. Chem. Interfacial Electrochem.* **1977**, *85*, 377.
(36) Brabec, V.; Christian, S. D.; Dryhurst, G. *J. Electroanal. Chem. Interfacial Electrochem.* **1977**, *85*, 389.
(37) Retter, U. *J. Electroanal. Chem. Interfacial Electrochem.* **1978**, *87*, 181.
(38) Brabec, V.; Christian, S. D.; Dryhurst, G. *Biophys. Chem.* **1978**, *7*, 253.
(39) Brabec, V.; Christian, S.; Dryhurst, G. *Biophys. Chem.* **1978**, *8*, 151.
(40) Brabec, V.; Christian, S. D.; Dryhurst, G. *Bioelectrochem. Bioenerg.* **1978**, *5*, 635.
(41) Krznarič, D.; Valenta, P.; Nürnberg, H. W.; Branica, M. *J. Electroanal. Chem. Interfacial Electrochem.* **1987**, *93*, 41.
(42) Temerk, Y. M.; Valenta, P. *J. Electroanal. Chem. Interfacial Electrochem.* **1978**, *93*, 57.
(43) Temerk, Y. M.; Valenta, P.; Nürnberg, H. W. *J. Electroanal. Chem. Interfacial Electrochem.* **1979**, *100*, 77.
(44) Brabec, V.; Kim, M. H.; Christian, S. D.; Dryhurst, G. *J. Electroanal. Chem. Interfacial Electrochem.* **1979**, *100*, 111.
(45) Kim, M. H.; Christian, S. D.; Dryhurst, G. *Bioelectrochem. Bioenerg.* **1979**, *6*, 165.
(46) Baker, J. G.; Christian, S. D.; Kim, M. H.; Dryhurst, G. *Biophys. Chem.* **1979**, *9*, 355.
(47) Temerk, Y. M. *Can. J. Chem.* **1979**, *57*, 1136.
(48) Retter, U. *J. Electroanal. Chem. Interfacial Electrochem.* **1980**, *106*, 371.
(49) Temerk, Y. M.; Valenta, P.; Nürnberg, H. W. *J. Electroanal. Chem. Interfacial Electrochem.* **1980**, *109*, 289.
(50) Vetterl, V.; Pokorny, J. *Bioelectrochem. Bioenerg.* **1980**, *7*, 517.
(51) Temerk, Y. M.; Valenta, P.; Nürnberg, H. W. *Bioelectrochem. Bioenerg.* **1980**, *7*, 705.
(52) Uehara, M.; Elving, P. J. *Bioelectrochem. Bioenerg.* **1981**, *8*, 523.
(53) Temerk, Y. M.; Kamal, M. M. *Bioelectrochem. Bioenerg.* **1981**, *8*, 671.
(54) Temerk, Y. M.; Valenta, P.; Nürnberg, H. W. *J. Electroanal. Chem. Interfacial Electrochem.* **1982**, *131*, 265.
(55) Retter, U.; Lohse, H. *J. Electroanal. Chem. Interfacial Electrochem.* **1982**, *134*, 243.
(56) Retter, U. *J. Electroanal. Chem. Interfacial Electrochem.* **1982**, *136*, 167.
(57) Sridharan, R.; de Levie, R. *J. Phys. Chem.* **1982**, *86*, 4489.
(58) Wrona, M. Z. *Bioelectrochem. Bioenerg.* **1983**, *10*, 169.
(59) Temerk, Y. M.; Kamal, M. M. *Bioelectrochem. Bioenerg.* **1983**, *11*, 457.
(60) Jursa, J.; Vetterl, V. *Bioelectrochem. Bioenerg.* **1984**, *12*, 137.
(61) Temerk, Y. M.; Ahmed, M. E.; Kamal, M. M. *Bioelectrochem. Bioenerg.* **1984**, *12*, 205.
(62) Retter, U. *J. Electroanal. Chem. Interfacial Electrochem.* **1984**, *165*, 221.

(63) Retter, U. *J. Electroanal. Chem. Interfacial Electrochem.* **1984**, *179*, 25.
(64) Quarin, G. *Electrochim. Acta* **1984**, *29*, 1707.
(65) Wandlowski, T.; Kretchmer, E. *J. Electroanal. Chem. Interfacial Electrochem.* **1986**, *209*, 203.
(66) Wandlowski, T.; Kretchmer, E.; Müller, E.; Kuschel, F.; Hoffmann, S.; von Lipinski, J. *J. Electroanal. Chem. Interfacial Electrochem.* **1986**, *213*, 339.
(67) Sridharan, R.; de Levie, R. *J. Electroanal. Chem. Interfacial Electrochem.* **1986**, *201*, 133.
(68) Srinivasan, R.; de Levie, R. *J. Electroanal. Chem. Interfacial Electrochem.* **1986**, *201*, 145.
(69) Saffarian, M. H.; Sridharan, R.; de Levie, R. *J. Electroanal. Chem. Interfacial Electrochem.* **1987**, *218*, 273.
(70) Sridharan, R.; de Levie, R. *J. Electroanal. Chem. Interfacial Electrochem.* **1987**, *218*, 287.
(71) Sridharan, R.; de Levie, R. *J. Electroanal. Chem. Interfacial Electrochem.* **1987**, *230*, 241.
(72) Kontoyannis, C.; Sridharan, R.; de Levie, R. *J. Electroanal. Chem. Interfacial Electrochem.* **1987**, *236*, 309.
(73) Kontoyannis, C.; de Levie, R. *J. Electroanal. Chem. Interfacial Electrochem.*, in press.
(74) Armstrong, R. D. *J. Electroanal. Chem. Interfacial Electrochem.* **1969**, *20*, 168.
(75) Akhmetov, N. K.; Kaganovich, R. I.; Damaskin, B. B.; Mambetkaziev, E. A. *Elektrokhimiya* **1978**, *14*, 1761.
(76) Meurêe, N.; Gierst, L. *Collect. Czech. Chem. Commun.* **1971**, *36*, 389.
(77) Narayan, R.; Hackerman, N. *J. Electrochem. Soc.* **1971**, *118*, 1426.
(78) Frumkin, A. N.; Grigoryev, N. B. *J. Electrochem. Soc.* **1972**, *119*, 1695.
(79) Pillai, K. C.; Waghorne, W. E. *J. Electroanal. Chem. Interfacial Electrochem.* **1981**, *125*, 487.
(80) Hills, G.; Silva, F. *J. Electroanal. Chem. Interfacial Electrochem.* **1982**, *137*, 387.
(81) Buess-Herman, C.; Gierst, L.; Gonze, M. *J. Electroanal. Chem. Interfacial Electrochem.* **1987**, *226*, 267.
(82) Lambert, J. P.; Gierst, L. *Chem. Ing. Tech.* **1972**, *4*, 219.
(83) Chevalet, J.; Rouelle, F.; Gierst, L.; Lambert, P. J. *J. Electroanal. Chem. Interfacial Electrochem.* **1972**, *39*, 201.
(84) Jenard, A.; Hurwitz, H. D. *J. Electroanal. Chem. Interfacial Electrochem.* **1976**, *70*, 27.
(85) Buess-Herman, C.; Gierst, L.; Vanlaethem-Meurêe, N. *J. Electroanal. Chem. Interfacial Electrochem.* **1981**, *123*, 1.
(86) Buess-Herman, C.; Vanlaethem-Meurêe, N.; Quarin, G.; Gierst, L. *J. Electroanal. Chem. Interfacial Electrochem.* **1981**, *123*, 21.
(87) Quarin, G.; Buess-Herman, C.; Gierst, L. *J. Electroanal. Chem. Interfacial Electrochem.* **1981**, *123*, 35.
(88) Gierst, L.; Franck, C.; Quarin, G.; Buess-Herman, C. *J. Electroanal. Chem. Interfacial Electrochem.* **1981**, *129*, 353.
(89) Buess-Herman, C.; Quarin, G.; Gierst, L.; Lipkowski, J. *J. Electroanal. Chem. Interfacial Electrochem.* **1983**, *148*, 79.
(90) Buess-Herman, C.; Quarin, G.; Gierst, L. *J. Electroanal. Chem. Interfacial Electrochem.* **1983**, *148*, 97.
(91) Thomas, F. G.; Gierst, L. *J. Electroanal. Chem. Interfacial Electrochem.* **1983**, *154*, 239.
(92) Buess-Herman, C.; Gierst, L. *Electrochim. Acta* **1984**, *29*, 303.
(93) Buess-Herman, C. *J. Electroanal. Chem. Interfacial Electrochem.* **1985**, *186*, 41.
(94) Buess-Herman, C.; Franck, C.; Gierst, L. *Electrochim. Acta* **1986**, *31*, 965.
(95) Lipkowski, J.; Buess-Herman, C.; Lambert, J. P.; Gierst, L. *J. Electroanal. Chem. Interfacial Electrochem.* **1986**, *202*, 169.
(96) Scheller, F.; Prümke, H. J.; Seyer, I. *J. Electroanal. Chem. Interfacial Electrochem.* **1976**, *67*, 241.
(97) Kůta, J.; Pospíšil, L.; Smoler, I. *J. Electroanal. Chem. Interfacial Electrochem.* **1977**, *75*, 407.
(98) Pospíšil, L.; Kůta, J.; Müller, E.; Dörfler, H.-D. *J. Electroanal. Chem. Interfacial Electrochem.* **1980**, *106*, 359.
(99) Müller, E.; Dörfler, H.-D. *Bioelectrochem. Bioenerg.* **1980**, *7*, 459.
(100) Pospíšil, L.; Müller, E.; Emons, H.; Dörfler, H.-D. *J. Electroanal. Chem. Interfacial Electrochem.* **1984**, *170*, 319.
(101) Pospíšil, L.; Müller, E.; Dörfler, H.-D. *Electrochim. Acta* **1984**, *29*, 773.
(102) Müller, E.; Emons, H.; Dörfler, H.-D. *Bioelectrochem. Bioenerg.* **1983**, *10*, 279.
(103) Kontoyannis, C.; Pospíšil, L.; de Levie, R. *J. Electroanal. Chem. Interfacial Electrochem.* **1987**, *222*, 277.
(104) Thomas, G.; Buess-Herman, C.; Gierst, L. *J. Electroanal. Chem. Interfacial Electrochem.* **1986**, *214*, 597.
(105) Srinivasan, R.; de Levie, R. *J. Phys. Chem.* **1987**, *91*, 2904.
(106) Srinivasan, R.; de Levie, R., in preparation.
(107) Frumkin, A. N.; Damaskin, B. B. *Dokl. Akad. Nauk SSSR* **1959**, *129*, 862.
(108) Damaskin, B. B.; Nikolaeva-Fedorovich, N. V. *Zh. Fiz. Khim.* **1961**, *35*, 1279.
(109) Srinivasan, R.; de Levie, R. *J. Electroanal. Chem. Interfacial Electrochem.* **1987**, *206*, 307.
(110) Mikhailik, Yu. V.; Damaskin, B. B. *Elektrokhimiya* **1979**, *15*, 566.
(111) Sridharan, R.; Saffarian, M. H.; de Levie, R. *J. Electroanal. Chem. Interfacial Electrochem.* **1987**, *236*, 311.
(112) Sridharan, R.; de Levie, R., in preparation.
(113) de Levie, R. *Adv. Electrochem. Electrochem. Eng.* **1985**, *13*, 1.
(114) Buess-Herman, C. In *Trends in Interfacial Electrochemistry*; Silva, A. F., Ed.; Reidel: Dordrecht, 1986; p 205.
(115) Fleischmann, M.; Thirsk, H. R. *Adv. Electrochem. Electrochem. Eng.* **1963**, *3*, 123.
(116) Canac, F. *C. R. Hebd. Seances Acad. Sci.* **1933**, *196*, 51.
(117) Kolmogorov, A. N. *Bull. Acad. Sci. URSR Cl. Sci. Math. Nat.* **1937**, *3*, 355.
(118) Avrami, M. *J. Chem. Phys.* **1940**, *8*, 212.
(119) Mampel, K. L. *Z. Phys. Chem.* **1940**, *A187*, 43.
(120) Evans, U. R. *Trans. Faraday Soc.* **1945**, *41*, 365.
(121) Jackson, J. *Trans. Faraday Soc.* **1940**, *36*, 1248.
(122) Schiffrin, D. J. *J. Electroanal. Chem. Interfacial Electrochem.* **1969**, *23*, 168.
(123) Lawrence, J.; Mohilner, D. M. *J. Electrochem. Soc.* **1971**, *118*, 259.
(124) Lawrence, J.; Mohilner, D. M. *J. Electrochem. Soc.* **1971**, *118*, 1596.
(125) Ozeki, K.; Sakabe, N.; Tanaka, J. *Acta Crystallogr., Sect. B: Struct. Crystallogr. Cryst. Chem.* **1969**, *B25*, 1038.
(126) Voet, D.; Rich, A. *Prog. Nucleic Acid Res. Mol. Biol.* **1970**, *10*, 183.
(127) Buess-Herman, C. *J. Electroanal. Chem. Interfacial Electrochem.* **1985**, *186*, 27.
(128) Peierls, R. E. *Helv. Chim. Acta* **1934**, *7* (Suppl. II), 81.
(129) Peierls, R. E. *Ann. Inst. Henri Pointcarê* **1935**, *5*, 177.
(130) Mermin, N. D. *Phys. Rev.* **1968**, *176*, 250.
(131) Kosterlitz, J. M. In *Phase Transitions in Surface Films*; Dash, J. G., Ruvalds, J., Eds.; Plenum: New York, 1980; p 193.
(132) Lippmann, G. *Ann. Chim. Phys.* **1875**, (5)5, 494.
(133) Koenig, F. O. *J. Phys. Chem.* **1934**, *38*, 111.
(134) Grahame, D. C.; Whitney, R. B. *J. Am. Chem. Soc.* **1942**, *64*, 1548.
(135) Volmer, M.; Weber, A. *Z. Phys. Chem.* **1926**, *119*, 227.
(136) Kaischev, R.; Stranski, I. N. *Z. Phys. Chem.* **1934**, *A170*, 195.
(137) Becker, R.; Döhring, W. *Ann. Phys.* **1935**, *416*, 719.
(138) Zeldovich, J. B. *Acta Physicochim. URSS* **1943**, *18*, 1.
(139) Buess-Herman, C. *J. Electroanal. Chem. Interfacial Electrochem.* **1985**, *186*, 41.
(140) Damaskin, B. B. *J. Electroanal. Chem. Interfacial Electrochem.* **1969**, *21*, 149.
(141) Damaskin, B. B. *Elektrokhimiya* **1977**, *13*, 816.
(142) Gurevich, Y.; Kharkats, Y. *J. Electroanal. Chem. Interfacial Electrochem.* **1978**, *86*, 245.
(143) Kharkats, Y. *J. Electroanal. Chem. Interfacial Electrochem.* **1980**, *115*, 75.
(144) Frumkin, A. N. *Z. Phys. Chem.* **1925**, *116*, 466.
(145) Lenz, W. *Phys. Z.* **1920**, *21*, 613.
(146) Ising, E. *Z. Phys.* **1925**, *31*, 253.
(147) Onsager, L. *Phys. Rev.* **1944**, (2)65, 117.
(148) Sridharan, R.; de Levie, R.; Rangarajan, S. K. *Chem. Phys. Lett.* **1987**, *142*, 43.
(149) Heyrovský, J. *Discuss. Faraday Soc.* **1947**, *1*, 212.
(150) de Levie, R. *J. Electrochem. Soc.* **1971**, *118*, 185C.
(151) Frumkin, A. N. *Z. Phys. Chem., Abt. A* **1933**, *164*, 121.
(152) Melik-Gaikazyan, V. I. *Zh. Fiz. Khim.* **1952**, *26*, 1184.
(153) Murray, R. W.; Gross, D. J. *Anal. Chem.* **1966**, *38*, 392.
(154) Gross, D. J.; Murray, R. W. *Anal. Chem.* **1966**, *38*, 405.
(155) Barker, G. C.; Bolzan, J. A. *Fresenius' Z. Anal. Chem.* **1966**, *216*, 215.
(156) Elliott, C. M.; Murray, R. W. *J. Am. Chem. Soc.* **1974**, *96*, 3321.
(157) Saffarian, M. H.; de Levie, R. *J. Electroanal. Chem. Interfacial Electrochem.* **1985**, *189*, 325.
(158) Peter, L. M.; Reid, J. D.; Scharifker, B. R. *J. Electroanal. Chem. Interfacial Electrochem.* **1981**, *119*, 73.
(159) Benucci, C.; Sharifker, B. R. *J. Electroanal. Chem. Interfacial Electrochem.* **1985**, *190*, 199.
(160) Müller, C.; Claret, J.; Martinez, F.; Sarret, M. *J. Electroanal. Chem. Interfacial Electrochem.* **1986**, *202*, 203.
(161) Müller, C.; Claret, J.; Sarret, M. *Electrochim. Acta* **1987**, *32*, 283.